

Effect of pseudogap on electronic Raman response in cuprate superconductors

Pengfei Jing and Yiqun Liu

Department of Physics, Beijing Normal University, Beijing 100875, China

Huaisong Zhao

College of Physics, Qingdao University, Qingdao 266071, China

Lülin Kuang

Sugon National Research Center for High-performance Computing Engineering Technology, Beijing 100093, China

Shiping Feng*

Department of Physics, Beijing Normal University, Beijing 100875, China

It has become clear that the anomalous properties of cuprate superconductors are intimately related to the formation of a pseudogap. Within the framework of the kinetic-energy-driven superconducting mechanism, the effect of the pseudogap on the electronic Raman response of cuprate superconductors in the superconducting-state is studied by taking into account the interplay between the superconducting gap and pseudogap. It is shown that the low-energy spectra almost rise as the cube of energy in the B_{1g} channel and linearly with energy in the B_{2g} channel. However, the pseudogap is strongly anisotropic in momentum space, where although the pseudogap never vanishes on the electron Fermi surface except for the hot spots, the magnitude of the pseudogap around the nodes is smaller than that around the antinodes, which leads to that the low-energy spectral weight of the B_{1g} spectrum is suppressed heavily by the pseudogap, while the pseudogap has a more modest effect on the electronic Raman response in the B_{2g} orientation.

PACS numbers: 74.72.Kf, 74.25.nd, 74.72.Gh, 74.20.Mn

It is now generally accepted that below a characteristic temperature T^* , which can be well above the superconducting (SC) transition temperature T_c in the underdoped and optimally doped regimes, the physical response of cuprate superconductors can be interpreted in terms of the formation of a pseudogap by which it means a suppression of the spectral weight of the low-energy quasiparticle excitations¹⁻³. This characteristic temperature T^* is so-called as the pseudogap crossover temperature. Below T^* the electronic state properties are very unusual¹⁻³. The origin of the pseudogap in cuprate superconductors remains a mystery second only to that of superconductivity itself, and it is widely believed that by the investigation of the former one might uncover essential insights for the understanding of the latter.

In order to fully understand the nature of the pseudogap state in cuprate superconductors, the two-particle Raman scattering experiments that can probe the quasiparticle dynamics on different regions of the Brillouin zone (BZ) have provided useful information for clarifying the nature of the pseudogap phase of cuprate superconductors^{3,4}. In a striking contrast to the infrared measurements of the conductivity spectrum², the electronic Raman scattering can be used to give directly two spectra B_{1g} and B_{2g} , each representing a different average over the electron Fermi surface (EFS)^{3,4}. After intensive investigations over more than two decades, it has been shown the electronic Raman response (ERR) spectrum in the SC-state is rather universal within the whole cuprate superconductors³⁻¹⁸, where the broad continuum scattering is depressed at low energies and the

spectral weight lost is transferred to higher energies, forming a broad peak whose position depends on the scattering geometry. In particular, the earliest evidence of the pseudogap effect manifested itself as a suppression of the SC-state ERR around the antinodal regime was observed on $\text{YBa}_2\text{Cu}_3\text{O}_{7-x}$ in the underdoped regime¹⁴. Later, these early observations have been further confirmed¹⁵⁻¹⁸, where a heavy loss in the spectral weight was found in the B_{1g} spectrum, and then the overall low-energy spectral weight in the B_{1g} spectrum is suppressed heavily by the pseudogap, however, only a light loss of the spectral weight was detected in the B_{2g} spectrum, indicating a strong momentum dependence of the pseudogap in cuprate superconductors. In this case, the electronic Raman scattering therefore gives the important information for the nature of the momentum dependence of the pseudogap which is not accessible via the conductivity measurement.

Theoretically, ERR of cuprate superconductors in the SC-state has been studied extensively^{3,4,19-24}. In particular, the ERR spectra in both the B_{1g} and B_{2g} orientations have been extracted to fit the electron-boson spectral density, and the results provide information on the angular variation of the electron self-energy and the corresponding spectral density around EFS²⁰. Moreover, it has been shown that ERR in the B_{1g} symmetry allows one to distinguish between phonon-mediated and magnetically mediated d-wave superconductivity²¹. However, to the best of our knowledge, the anisotropic suppression of the ERR spectrum by the momentum dependence of the pseudogap in cuprate superconductors has

not been treated starting from a microscopic theory. In this paper, we study the pseudogap-induced anisotropic suppression of the ERR spectrum in cuprate superconductors in the SC-state by considering the interplay between the pseudogap and SC gap. Within the framework of the kinetic-energy-driven SC mechanism²⁵⁻²⁷, we calculate the ERR function in terms of the Raman density-density correlation function, and then the obtained results show that the low-energy B_{2g} response depends linearly on energy ω , while the low-energy B_{1g} spectrum varies as ω^3 . However, our results also show that the pseudogap on EFS is strong momentum dependence, with the actual minimum that does not appear around the nodes, but locates exactly at the hot spots, where the pseudogap is equal to zero. In particular, the magnitude of the pseudogap around the nodes is smaller than that around the antinodes. This special structure of the momentum dependence of the pseudogap therefore leads to that the low-energy spectral weight of the B_{1g} spectrum is suppressed heavily by the pseudogap, while the pseudogap has a more modest effect on the ERR spectrum in the B_{2g} orientation.

ERR is manifested itself by the dynamical Raman response function $\tilde{S}(\omega)$, which can be obtained directly from the imaginary part of the Raman density-density correlation function $\tilde{\chi}(\mathbf{q}, \omega)$ as⁴,

$$\tilde{S}(\omega) = -\frac{1}{\pi}[1 + n_B(\omega)]\text{Im}\tilde{\chi}(\mathbf{q} \sim 0, \omega), \quad (1)$$

where $n_B(\omega)$ is the boson distribution function, while the Raman density-density correlation function $\tilde{\chi}(\mathbf{q}, \omega)$ is defined as,

$$\tilde{\chi}(\mathbf{q}, \tau - \tau') = -\langle T \rho_\gamma(\mathbf{q}, \tau) \rho_\gamma(-\mathbf{q}, \tau') \rangle, \quad (2)$$

where the Raman density operator in the Nambu representation can be expressed as,

$$\rho_\gamma(\mathbf{q}) = \sum_{\mathbf{k}} \gamma_{\mathbf{k}+\frac{\mathbf{q}}{2}}^\alpha C_{\mathbf{k}+\mathbf{q}}^\dagger \tau_3 C_{\mathbf{k}}, \quad (3)$$

with the Pauli matrix τ_3 , and the bare Raman vertex $\gamma_{\mathbf{k}}^\alpha$ that has been classified by the representations B_{1g} and B_{2g} of the point group D_{4h} as⁴,

$$\gamma_{\mathbf{k}}^{B_{1g}} = \frac{1}{4} b_{\omega_i, \omega_s} [\cos(k_x) - \cos(k_y)], \quad (4a)$$

$$\gamma_{\mathbf{k}}^{B_{2g}} = b'_{\omega_i, \omega_s} \sin(k_x) \sin(k_y), \quad (4b)$$

respectively, where as a qualitative discussion, the magnitude of the energy dependence of the prefactors b and b' can be rescaled to units. In cuprate superconductors, the B_{1g} spectrum samples the antinodal region, the Fermi momentum on the BZ boundary, while the B_{2g} spectrum samples the nodal region, therefore ERR probes complementary regimes of EFS⁴. Substituting the Raman density operator (3) into Eq. (2), the Raman density-density correlation function $\tilde{\chi}(\mathbf{q}, \omega)$ therefore can be rewritten in

terms of the single-electron Green's function $\mathbb{G}(\mathbf{k}, \omega)$ in the Nambu representation as,

$$\begin{aligned} \tilde{\chi}(\mathbf{q}, iq_m) &= \frac{1}{N} \sum_{\mathbf{k}} \gamma_{\mathbf{k}+\frac{\mathbf{q}}{2}}^\alpha \gamma_{2\mathbf{k}+\frac{\mathbf{q}}{2}}^\alpha \\ &\times \frac{1}{\beta} \sum_{i\omega_n} \text{Tr}[\mathbb{G}(\mathbf{k} + \mathbf{q}, i\omega_n + iq_m) \tau_3 \mathbb{G}(\mathbf{k}, i\omega_n) \tau_3]. \end{aligned} \quad (5)$$

It should be emphasized that in the obtaining above Raman density-density correlation function, the vertex correction has been ignored, since it has been shown that the vertex correction in the pseudogap phase is negligibly small^{28,29}. Eq. (5) also indicates that for the evaluation of the electronic Raman density-density correlation function in the SC-state, we firstly need to obtain the single-electron Green's function.

The t - J model on a square-lattice is widely accepted for the description of the essential physics of cuprate superconductors^{30,31}. This t - J model is defined as,

$$H = - \sum_{ll'} t_{ll'} C_{l\sigma}^\dagger C_{l'\sigma} + \mu \sum_{l\sigma} C_{l\sigma}^\dagger C_{l\sigma} + J \sum_{\langle ll' \rangle} S_l \cdot S_{l'}, \quad (6)$$

supplemented by an important on-site local constraint to avoid the double occupancy, $\sum_{\sigma} C_{l\sigma}^\dagger C_{l\sigma} \leq 1$, where $C_{l\sigma}^\dagger$ ($C_{l\sigma}$) is the electron creation (annihilation) operator with spin σ on the lattice site l , S_l is a spin operator located on the lattice site l , μ is the chemical potential, J is the exchange interaction between the nearest-neighbor (NN) sites on a square-lattice, and the summation $\langle ll' \rangle$ is carried over the NN bonds. For the hopping $t_{ll'}$, we take only t for the NN hopping amplitude and $-t'$ for the next NN hopping amplitude, respectively. In this paper, these parameters are chosen as $t/J = 2.5$ and $t'/t = 0.3$. The strong electron correlation in the t - J model (6) manifests itself by the no-double electron occupancy local constraint³²⁻³⁶, which can be treated properly in actual calculations within the framework of the charge-spin separation fermion-spin theory^{27,37}, where the constrained electron is decoupled as a charge carrier and a localized spin, with the charge carrier that represents the charge degree of freedom together with some effects of spin configuration rearrangements due to the presence of the doped charge carrier itself, while the localized spin represents the spin degree of freedom. Based on the t - J model in the fermion-spin representation, the kinetic-energy-driven SC mechanism has been developed²⁵⁻²⁷, where the interaction between the charge carriers and spin directly from the kinetic energy by the exchange of spin excitations generates the SC-state in the particle-particle channel and pseudogap state in the particle-hole channel, therefore there is an interplay between the SC gap and pseudogap in the whole SC dome²⁶.

In the framework of the charge-spin separation, the single-electron Green's function is obtained in terms of the charge-spin recombination³²⁻³⁶. Recently, we³⁸ have developed a full charge-spin recombination scheme to fully recombine a charge carrier and a localized spin into

a constrained electron, where the obtained electron propagator can give a consistent description of the nature of EFS in cuprate superconductors. In the following discussions, we reproduce only the main details in the calculations of the single-electron Green's function of the

t - J model under the fermion-spin representation in the SC-state. In Ref. 38, the single-electron diagonal and off-diagonal Green's functions of the t - J model in the SC-state have been obtained in terms of the full charge-spin recombination scheme as,

$$G(\mathbf{k}, \omega) = \frac{\omega + \varepsilon_{\mathbf{k}} + \Sigma_1(\mathbf{k}, -\omega)}{[\omega - \varepsilon_{\mathbf{k}} - \Sigma_1(\mathbf{k}, \omega)][\omega + \varepsilon_{\mathbf{k}} + \Sigma_1(\mathbf{k}, -\omega)] - \bar{\Delta}^2(\mathbf{k})}, \quad (7a)$$

$$\Im^\dagger(\mathbf{k}, \omega) = -\frac{\bar{\Delta}(\mathbf{k})}{[\omega - \varepsilon_{\mathbf{k}} - \Sigma_1(\mathbf{k}, \omega)][\omega + \varepsilon_{\mathbf{k}} + \Sigma_1(\mathbf{k}, -\omega)] - \bar{\Delta}^2(\mathbf{k})}, \quad (7b)$$

where the bare electron excitation spectrum $\varepsilon_{\mathbf{k}} = -Zt\gamma_{\mathbf{k}} + Zt'\gamma'_{\mathbf{k}} + \mu$, with $\gamma_{\mathbf{k}} = (\cos k_x + \cos k_y)/2$, $\gamma'_{\mathbf{k}} = \cos k_x \cos k_y$, Z is the number of the NN or next NN sites on a square lattice, and the d-wave SC gap $\bar{\Delta}(\mathbf{k}) = \Sigma_2(\mathbf{k}, \omega = 0) = \bar{\Delta}\gamma_{\mathbf{k}}^{(d)}$ with $\gamma_{\mathbf{k}}^{(d)} = (\cos k_x - \cos k_y)/2$,

while the electron self-energies $\Sigma_1(\mathbf{k}, \omega)$ in the particle-hole channel and $\Sigma_2(\mathbf{k}, \omega)$ in the particle-particle channel due to the interaction between electrons by the exchange of spin excitations have been obtained explicitly in terms of the spin bubble as³⁸,

$$\begin{aligned} \Sigma_1(\mathbf{k}, \omega) = & \frac{1}{2N^2} \sum_{\mathbf{p}\mathbf{p}'\nu\mu} (-1)^{\nu+1} \Omega_{\mathbf{p}\mathbf{p}'\mathbf{k}} \left[\left(1 + \frac{\bar{\varepsilon}_{\mathbf{p}+\mathbf{k}}}{E_{\mathbf{p}+\mathbf{k}}} \right) \frac{F_{\mu\mathbf{p}\mathbf{p}'\mathbf{k}}^{(\nu)}}{\omega - (-1)^\mu \omega_{\nu\mathbf{p}\mathbf{p}'} - E_{\mathbf{p}+\mathbf{k}}} \right. \\ & \left. + \left(1 - \frac{\bar{\varepsilon}_{\mathbf{p}+\mathbf{k}}}{E_{\mathbf{p}+\mathbf{k}}} \right) \frac{F_{\mu\mathbf{p}\mathbf{p}'\mathbf{k}}^{(\nu)}}{\omega + (-1)^\mu \omega_{\nu\mathbf{p}\mathbf{p}'} + E_{\mathbf{p}+\mathbf{k}}} \right], \end{aligned} \quad (8a)$$

$$\Sigma_2(\mathbf{k}, \omega) = \frac{1}{N^2} \sum_{\mathbf{p}\mathbf{p}'\nu\mu} (-1)^\nu \Omega_{\mathbf{p}\mathbf{p}'\mathbf{k}} \frac{\bar{\Delta}_Z(\mathbf{p}+\mathbf{k})}{2E_{\mathbf{p}+\mathbf{k}}} \left[\frac{F_{\mu\mathbf{p}\mathbf{p}'\mathbf{k}}^{(\nu)}}{\omega - (-1)^\mu \omega_{\nu\mathbf{p}\mathbf{p}'} - E_{\mathbf{p}+\mathbf{k}}} - \frac{F_{\mu\mathbf{p}\mathbf{p}'\mathbf{k}}^{(\nu)}}{\omega + (-1)^\mu \omega_{\nu\mathbf{p}\mathbf{p}'} + E_{\mathbf{p}+\mathbf{k}}} \right], \quad (8b)$$

respectively, where $\nu(\mu) = 1, 2$, $\bar{\varepsilon}_{\mathbf{k}} = Z_F \varepsilon_{\mathbf{k}}$, $\bar{\Delta}_Z(\mathbf{k}) = Z_F \bar{\Delta}(\mathbf{k})$, the SC quasiparticle energy spectrum $E_{\mathbf{k}} = \sqrt{\bar{\varepsilon}_{\mathbf{k}}^2 + |\bar{\Delta}_Z(\mathbf{k})|^2}$, $\Omega_{\mathbf{p}\mathbf{p}'\mathbf{k}} = Z_F \Lambda_{\mathbf{p}+\mathbf{p}'+\mathbf{k}}^2 B_{\mathbf{p}'} B_{\mathbf{p}+\mathbf{p}'}/(4\omega_{\mathbf{p}'} \omega_{\mathbf{p}+\mathbf{p}'})$, $\Lambda_{\mathbf{k}} = Zt\gamma_{\mathbf{k}} - Zt'\gamma'_{\mathbf{k}}$, the single-particle coherent weight $Z_F^{-1} = 1 - \text{Re}\Sigma_{10}(\mathbf{k}, \omega = 0) |_{\mathbf{k}=[\pi, 0]}$ with $\Sigma_{10}(\mathbf{k}, \omega)$ that is the antisymmetric part of the electron self-energy $\Sigma_1(\mathbf{k}, \omega)$, $\omega_{\nu\mathbf{p}\mathbf{p}'} = \omega_{\mathbf{p}+\mathbf{p}'} - (-1)^\nu \omega_{\mathbf{p}'}$, the functions, $F_{1\mathbf{p}\mathbf{p}'\mathbf{k}}^{(\nu)} = n_F(E_{\mathbf{p}+\mathbf{k}}) n_{1\mathbf{B}\mathbf{p}\mathbf{p}'}^{(\nu)} + n_{2\mathbf{B}\mathbf{p}\mathbf{p}'}^{(\nu)}$, $F_{2\mathbf{p}\mathbf{p}'\mathbf{k}}^{(\nu)} = [1 - n_F(E_{\mathbf{p}+\mathbf{k}})] n_{1\mathbf{B}\mathbf{p}\mathbf{p}'}^{(\nu)} + n_{2\mathbf{B}\mathbf{p}\mathbf{p}'}^{(\nu)}$, with $n_{1\mathbf{B}\mathbf{p}\mathbf{p}'}^{(\nu)} = 1 + n_B(\omega_{\mathbf{p}'+\mathbf{p}}) + n_B[(-1)^{\nu+1} \omega_{\mathbf{p}'}]$, $n_{2\mathbf{B}\mathbf{p}\mathbf{p}'}^{(\nu)} = n_B(\omega_{\mathbf{p}'+\mathbf{p}}) n_B[(-1)^{\nu+1} \omega_{\mathbf{p}'}]$, and the fermion distribution function $n_F(\omega)$, while the mean-field (MF) spin excitation spectrum $\omega_{\mathbf{k}}$ and function $B_{\mathbf{k}}$ have been given explicitly in Ref. 27.

As in our previous discussions³⁸, the electron self-energy $\Sigma_1(\mathbf{k}, \omega)$ in Eq. (8a) in the particle-hole channel is directly related to the momentum dependence of the

pseudogap as,

$$\Sigma_1(\mathbf{k}, \omega) \approx \frac{[\bar{\Delta}_{\text{PG}}(\mathbf{k})]^2}{\omega + \varepsilon_{0\mathbf{k}}}, \quad (9)$$

where the energy spectrum $\varepsilon_{0\mathbf{k}} = L_2^{(e)}(\mathbf{k})/L_1^{(e)}(\mathbf{k})$, the pseudogap $\bar{\Delta}_{\text{PG}}(\mathbf{k}) = L_2^{(e)}(\mathbf{k})/\sqrt{L_1^{(e)}(\mathbf{k})}$, while the functions $L_1^{(e)}(\mathbf{k}) = -\Sigma_{10}(\mathbf{k}, \omega = 0)$ and $L_2^{(e)}(\mathbf{k}) = \Sigma_1(\mathbf{k}, \omega = 0)$ can be obtained directly from $\Sigma_1(\mathbf{k}, \omega)$ in Eq. (8a).

Substituting the self-energy $\Sigma_1(\mathbf{k}, \omega)$ in Eq. (9) into Eq. (7), we therefore obtain the single-electron diagonal and off-diagonal Green's functions explicitly as,

$$G(\mathbf{k}, \omega) = \sum_{\nu=1,2} \left(\frac{U_{\nu\mathbf{k}}^2}{\omega - E_{\nu\mathbf{k}}} + \frac{V_{\nu\mathbf{k}}^2}{\omega + E_{\nu\mathbf{k}}} \right), \quad (10a)$$

$$\Im^\dagger(\mathbf{k}, \omega) = -\sum_{\nu=1,2} \frac{a_{\nu\mathbf{k}} \bar{\Delta}(\mathbf{k})}{2E_{\nu\mathbf{k}}} \left(\frac{1}{\omega - E_{\nu\mathbf{k}}} - \frac{1}{\omega + E_{\nu\mathbf{k}}} \right), \quad (10b)$$

where $a_{1\mathbf{k}} = (E_{1\mathbf{k}}^2 - \varepsilon_{0\mathbf{k}}^2)/(E_{1\mathbf{k}}^2 - E_{2\mathbf{k}}^2)$, $a_{2\mathbf{k}} = (E_{2\mathbf{k}}^2 - \varepsilon_{0\mathbf{k}}^2)/(E_{1\mathbf{k}}^2 - E_{2\mathbf{k}}^2)$, and then the SC quasiparticle spec-

trum has been split into two branches due to the presence of the pseudogap, $E_{1\mathbf{k}} = \sqrt{[\Phi_{1\mathbf{k}} + \Phi_{2\mathbf{k}}]/2}$ and $E_{2\mathbf{k}} = \sqrt{[\Phi_{1\mathbf{k}} - \Phi_{2\mathbf{k}}]/2}$, with the kernel functions, $\Phi_{1\mathbf{k}} = \varepsilon_{\mathbf{k}}^2 + \varepsilon_{0\mathbf{k}}^2 + 2\bar{\Delta}_{\text{PG}}^2(\mathbf{k}) + \bar{\Delta}^2(\mathbf{k})$, $\Phi_{2\mathbf{k}} = \sqrt{(\varepsilon_{\mathbf{k}}^2 - \varepsilon_{0\mathbf{k}}^2)b_{1\mathbf{k}} + 4\bar{\Delta}_{\text{PG}}^2(\mathbf{k})b_{2\mathbf{k}} + \bar{\Delta}^4(\mathbf{k})}$, $b_{1\mathbf{k}} = \varepsilon_{\mathbf{k}}^2 - \varepsilon_{0\mathbf{k}}^2 + 2\bar{\Delta}^2(\mathbf{k})$, and $b_{2\mathbf{k}} = (\varepsilon_{\mathbf{k}} - \varepsilon_{0\mathbf{k}})^2 + \bar{\Delta}^2(\mathbf{k})$, while the coherence factors,

$$\begin{aligned} U_{1\mathbf{k}}^2 &= \frac{1}{2} \left[a_{1\mathbf{k}} \left(1 + \frac{\varepsilon_{\mathbf{k}}}{E_{1\mathbf{k}}} \right) - a_{3\mathbf{k}} \left(1 + \frac{\varepsilon_{0\mathbf{k}}}{E_{1\mathbf{k}}} \right) \right], \\ V_{1\mathbf{k}}^2 &= \frac{1}{2} \left[a_{1\mathbf{k}} \left(1 - \frac{\varepsilon_{\mathbf{k}}}{E_{1\mathbf{k}}} \right) - a_{3\mathbf{k}} \left(1 - \frac{\varepsilon_{0\mathbf{k}}}{E_{1\mathbf{k}}} \right) \right], \\ U_{2\mathbf{k}}^2 &= -\frac{1}{2} \left[a_{2\mathbf{k}} \left(1 + \frac{\varepsilon_{\mathbf{k}}}{E_{2\mathbf{k}}} \right) - a_{3\mathbf{k}} \left(1 + \frac{\varepsilon_{0\mathbf{k}}}{E_{2\mathbf{k}}} \right) \right], \\ V_{2\mathbf{k}}^2 &= -\frac{1}{2} \left[a_{2\mathbf{k}} \left(1 - \frac{\varepsilon_{\mathbf{k}}}{E_{2\mathbf{k}}} \right) - a_{3\mathbf{k}} \left(1 - \frac{\varepsilon_{0\mathbf{k}}}{E_{2\mathbf{k}}} \right) \right], \end{aligned}$$

satisfy the sum rule: $U_{1\mathbf{k}}^2 + V_{1\mathbf{k}}^2 + U_{2\mathbf{k}}^2 + V_{2\mathbf{k}}^2 = 1$, where $a_{3\mathbf{k}} = \bar{\Delta}_{\text{PG}}^2(\mathbf{k})/(E_{1\mathbf{k}}^2 - E_{2\mathbf{k}}^2)$.

Substituting the Green's function (10) into Eqs. (5) and (1), the ERR function $\tilde{S}(\omega)$ is therefore obtained explicitly as,

$$\begin{aligned} \tilde{S}(\omega) &= [1 + n_B(\omega)] \frac{2}{N} \sum_{\mathbf{k}\mu\nu} \gamma_{1\mathbf{k}}^\alpha \gamma_{2\mathbf{k}}^\alpha \{ L_{\mu\nu}^{(1)}(\mathbf{k}) \\ &\times [A_{\mu\nu}^{(1)}(\mathbf{k})\delta(\omega + E_{\nu\mathbf{k}} - E_{\mu\mathbf{k}}) \\ &- A_{\mu\nu}^{(2)}(\mathbf{k})\delta(\omega - E_{\nu\mathbf{k}} + E_{\mu\mathbf{k}})] \\ &+ L_{\mu\nu}^{(2)}(\mathbf{k})[A_{\mu\nu}^{(3)}(\mathbf{k})\delta(\omega - E_{\nu\mathbf{k}} - E_{\mu\mathbf{k}}) \\ &- A_{\mu\nu}^{(4)}(\mathbf{k})\delta(\omega + E_{\nu\mathbf{k}} + E_{\mu\mathbf{k}})] \}, \end{aligned} \quad (11)$$

where $L_{\mu\nu}^{(1)}(\mathbf{k}) = n_{\text{F}}(E_{\nu\mathbf{k}}) - n_{\text{F}}(E_{\mu\mathbf{k}})$, $L_{\mu\nu}^{(2)}(\mathbf{k}) = 1 - n_{\text{F}}(E_{\nu\mathbf{k}}) - n_{\text{F}}(E_{\mu\mathbf{k}})$, $A_{\mu\nu}^{(1)}(\mathbf{k}) = U_{\mu\mathbf{k}}^2 U_{\nu\mathbf{k}}^2 - \Xi_{\mu\nu}(\mathbf{k})$, $A_{\mu\nu}^{(2)}(\mathbf{k}) = V_{\mu\mathbf{k}}^2 V_{\nu\mathbf{k}}^2 - \Xi_{\mu\nu}(\mathbf{k})$, $A_{\mu\nu}^{(3)}(\mathbf{k}) = U_{\mu\mathbf{k}}^2 V_{\nu\mathbf{k}}^2 - \Xi_{\mu\nu}(\mathbf{k})$, $A_{\mu\nu}^{(4)}(\mathbf{k}) = V_{\mu\mathbf{k}}^2 U_{\nu\mathbf{k}}^2 - \Xi_{\mu\nu}(\mathbf{k})$, and $\Xi_{\mu\nu}(\mathbf{k}) = a_{\mu\mathbf{k}} a_{\nu\mathbf{k}} \bar{\Delta}^2(\mathbf{k})/(4E_{\mu\mathbf{k}} E_{\nu\mathbf{k}})$.

We are now ready to discuss ERR of cuprate superconductors in the SC-state. However, in the following discussions, we only focus on the low-energy features related to the anisotropic suppression of the low-energy spectral weight by the momentum dependence of the pseudogap. As a comparison of the results between the cases of the presence and absence of the pseudogap, we firstly discuss the case of the absence of the pseudogap, i.e., $\bar{\Delta}_{\text{PG}} = 0$. In this case, the ERR function $\tilde{S}(\omega)$ in Eq. (11) is reduced as,

$$\begin{aligned} \tilde{S}^{(0)}(\mathbf{q}, \omega) &= [1 + n_B(\omega)] \frac{1}{2N} \sum_{\mathbf{k}} \gamma_{1\mathbf{k}}^\alpha \gamma_{2\mathbf{k}}^\alpha \frac{\bar{\Delta}^2(\mathbf{k})}{E_{\mathbf{k}}^{(0)2}} \\ &\times \text{th} \left(\frac{1}{2} \beta E_{\mathbf{k}}^{(0)} \right) [\delta(\omega - 2E_{\mathbf{k}}^{(0)}) - \delta(\omega + 2E_{\mathbf{k}}^{(0)})], \end{aligned} \quad (12)$$

with $E_{\mathbf{k}}^{(0)} = \sqrt{\varepsilon_{\mathbf{k}}^2 + |\bar{\Delta}(\mathbf{k})|^2}$. We have performed a calculation for the ERR function (12) in both B_{1g} and B_{2g}

orientations, and the results of the B_{1g} and B_{2g} spectra (dash-dotted line) at doping $\delta = 0.15$ with temperature $T = 0.002J$ are plotted in Fig. 1a and Fig. 1b, respectively, where both B_{1g} and B_{2g} spectra are characterized clearly by the presence of the pair-breaking peaks, however, the peak in the B_{1g} spectrum is located around the energy $\omega = 2\bar{\Delta}$, while the intensity of the B_{2g} spectrum is weaker than the B_{1g} one and the peak position is located at a lower energy³⁻¹³.

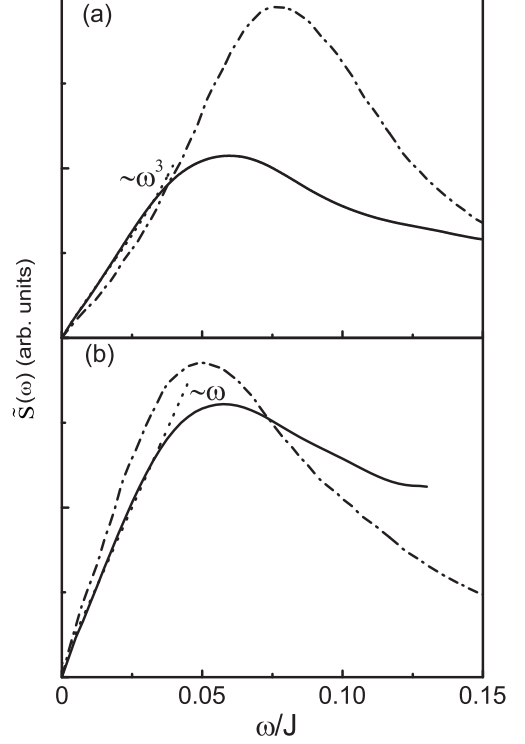


FIG. 1: (a) B_{1g} and (b) B_{2g} spectra (solid line) as a function of energy at $\delta = 0.15$ with $T = 0.002J$ for $t/J = 2.5$ and $t'/t = 0.3$. The dotted lines are a cubic and a linear fits for the low-energy B_{1g} and B_{2g} spectra, respectively. For comparison, the corresponding results of the B_{1g} and B_{2g} spectra in the case of the absence of the pseudogap (dash-dotted lines) are also shown in (a) and (b), respectively.

However, when the pseudogap effect is included in terms of the electron self-energy $\Sigma_1(\mathbf{k}, \omega)$, the spectral weight of the ERR spectrum is suppressed. To see this point clearly, we also plot the results of the B_{1g} and B_{2g} spectra (solid line) in case of the presence of the pseudogap $\bar{\Delta}_{\text{PG}}$ obtained from the Eq. (11) at $\delta = 0.15$ with $T = 0.002J$ in Fig. 1a and Fig. 1b, respectively. In comparison with the corresponding results in the absence of the pseudogap (dash-dotted line), we therefore find that although the low-energy spectral weight of the ERR spectrum in the both B_{1g} and B_{2g} symmetries has been redistributed, the low-energy spectral weight in the B_{1g} channel is suppressed heavily by the pseudogap, while the spectral weight in the B_{2g} channel is reduced lightly, in qualitative agreement with the experimental data¹⁴⁻¹⁸. In particular, we have also calculated the energy depen-

dence of the ERR functions up to higher energies, and the results show that the redistribution of the spectral weight induced by the pseudogap leads to a transfer of the missing low-energy spectral weight to the higher-energy region^{8,14–18}. Moreover, a numerical fit has been made to the low-energy data, and the results show that in the depleted low-energy region of the B_{2g} spectrum, the intensity rises linearly with energy ω , while the low-energy spectrum varies as ω^3 in the B_{1g} channel (see the dotted line in Fig. 1), which are also consistent with the experimental data^{3–18}, however, are in a striking contrast to the conventional superconductors, where the ERR spectrum in the low-energy regime for an isotropic s-wave gap is characterized by the exponentially activated behavior. Furthermore, we have made a series of calculations for the B_{2g} spectrum at different doping levels, and the results show that the B_{2g} spectrum has a domelike shape of the doping dependence, and actually scales with T_c throughout the doping range.

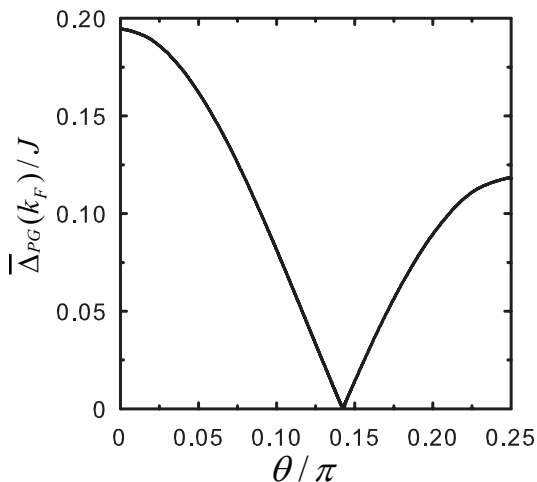


FIG. 2: The angular dependence of the pseudogap on the electron Fermi surface at $\delta = 0.15$ with $T = 0.002J$ for $t/J = 2.5$ and $t'/t = 0.3$.

The poles of the electron Green's function (7a) at zero energy determine directly EFS in momentum space, while the everything happens at EFS. An explanation of the anisotropic suppressions of ERR in cuprate superconductors in the SC-state can be found from the electron self-energy $\Sigma_1(\mathbf{k}, \omega)$ in Eq. (9) in the particle-hole channel, where the momentum dependence of the pseudogap is related explicitly to the electron scattering as $\text{Im}\Sigma_1(\mathbf{k}, \omega) \approx 2\pi[\bar{\Delta}_{PG}(\mathbf{k})]^2\delta(\omega + \varepsilon_{0\mathbf{k}})$, also reflecting a fact that the product of $[\bar{\Delta}_{PG}(\mathbf{k}_F)]^2$ and the delta function $\delta(\varepsilon_{0\mathbf{k}_F})$ has the same momentum dependence on EFS

as that of $|\text{Im}\Sigma_1(\mathbf{k}_F)|$. To show the momentum dependence of the pseudogap on EFS clearly, we plot the angular dependence of the pseudogap $\bar{\Delta}_{PG}(\mathbf{k}_F)$ on EFS at $\delta = 0.15$ with $T = 0.002J$ in Fig. 2, where the pseudogap $\bar{\Delta}_{PG}(\mathbf{k}_F)$ is strongly anisotropic in momentum space. The most striking feature is that the actual minimum of the pseudogap does not appear around the node, but locates exactly at the hot spot \mathbf{k}_{HS} , where the pseudogap $\bar{\Delta}_{PG}(\mathbf{k}_{HS}) = 0$, and then the charge-order state is driven by the Fermi-arc instability, with a characteristic wave vector corresponding to the hot spots of EFS^{39–45}. This pseudogap opening around the node is also consistent with the experimental observations^{18,46}. On the other hand, the magnitude of the pseudogap $\bar{\Delta}_{PG}(\mathbf{k}_F)$ still exhibits the largest value around the antinode, and then it decreases with the move of the momentum away from the antinode. In particular, the magnitude of the pseudogap around the node is smaller than that around the antinode. This special momentum dependence of the pseudogap therefore suppresses heavily the low-energy spectral weight of B_{1g} spectrum, but has a more modest effect on ERR in the B_{2g} channel.

In conclusion, within the framework of the kinetic-energy-driven SC mechanism, we have studied pseudogap effect on the ERR spectrum in cuprate superconductors in the SC-state by taking into account the interplay between the pseudogap and SC gap. Our results show that the low-energy B_{2g} spectrum depends linearly on energy ω , while the low-energy B_{1g} spectrum displays a cube energy dependence. In particular, the pseudogap is strong momentum dependence, where although the pseudogap never vanishes on EFS except for the hot spots, the magnitude of the pseudogap around the nodes is smaller than that around the antinodes. This special structure of the pseudogap therefore leads to that the low-energy spectral weight in the B_{1g} orientation is suppressed heavily by the pseudogap, while the pseudogap has a more modest effect on ERR in the B_{2g} channel. Our these theoretical results are in qualitative agreement with the experimental data.

Acknowledgments

The authors would like to thank Deheng Gao and Jinping Mou for helpful discussions. P.J, YL, LK, and SF are supported by the National Key Research and Development Program of China under Grant No. 2016YFA0300304, and National Natural Science Foundation of China (NSFC) under Grant No. 11574032, and HZ is supported by NSFC under Grant No. 11547034.

* Electronic address: spfeng@bnu.edu.cn

¹ See, e.g., the review, S. Hüfner, M. A. Hossain, A. Damascelli, and G. A. Sawatzky, Rep. Prog. Phys. **71**, 062501

(2008).

² See, e.g., the review, D. N. Basov and T. Timusk, Rev. Mod. Phys. **77**, 721 (2005).

- ³ See, e.g., the review, Tom Timusk and Bryan Statt, Rep. Prog. Phys. **62**, 61 (1999), and references therein.
- ⁴ See, e.g., the review, T. P. Devereaux and R. Hackl, Rev. Mod. Phys. **79**, 175 (2007), and references therein.
- ⁵ T. Staufer, R. Nemetschek, R. Hackl, P. Müller, and H. Veith, Phys. Rev. Lett. **68**, 1069 (1992).
- ⁶ X. K. Chen, J. C. Irwin, H. J. Trodahl, T. Kimura, and K. Kishio, Phys. Rev. Lett. **73**, 3290 (1994); X. K. Chen, J. C. Irwin, H. J. Trodahl, M. Okuya, T. Kimura, and K. Kishio, Physica C **295**, 80 (1998).
- ⁷ F. Venturini, M. Opel, R. Hackl, H. Berger, L. Forró, and B. Revaz, J. Phys. Chem. Solids **63**, 2345 (2002).
- ⁸ K. C. Hewitt and J. C. Irwin, Phys. Rev. B **66**, 054516 (2002).
- ⁹ M. Le Tacon, A. Sacuto, A. Georges, G. Kotliar, Y. Gallais, D. Colson, and A. Forget, Nature Phys. **2**, 537 (2006).
- ¹⁰ W. Guyard, A. Sacuto, M. Cazayous, Y. Gallais, M. Le Tacon, D. Colson, and A. Forget, Phys. Rev. Lett. **101**, 097003 (2008); W. Guyard, M. Le Tacon, M. Cazayous, A. Sacuto, A. Georges, D. Colson, and A. Forget, Phys. Rev. B **77**, 024524 (2008).
- ¹¹ S. Blanc, Y. Gallais, A. Sacuto, M. Cazayous, M. A. Méasson, G. D. Gu, J. S. Wen, and Z. J. Xu, Phys. Rev. B **80**, 140502(R) (2009).
- ¹² W. Prestel, F. Venturini, B. Muschler, I. Tütto, R. Hackl, M. Lambacher, A. Erb, Seiki Komiyama, Shimpei Ono, Yoichi Ando, D. Inosov, V.B. Zabolotnyy, and S. V. Borisenko, Eur. Phys. J. ST. **188**, 163 (2010).
- ¹³ B. Loret, S. Sakai, Y. Gallais, M. Cazayous, M.-A. Méasson, A. Forget, D. Colson, M. Civelli, and A. Sacuto, Phys. Rev. Lett. **116**, 197001 (2016)
- ¹⁴ R. Nemetschek, M. Opel, C. Hoffmann, P. F. Müller, R. Hackl, H. Berger, L. Forró, A. Erb, and E. Walker, Phys. Rev. Lett. **78**, 4837 (1997).
- ¹⁵ J G Naeini, J C Irwin, T Sasagawa, Y Togawa, and K Kishio, Can. J. Phys. **78**, 483 (2000).
- ¹⁶ M. Opel, R. Nemetschek, C. Hoffmann, R. Philipp, P. F. Müller, R. Hackl, I. Tüttó, A. Erb, B. Revaz, E. Walker, H. Berger, and L. Forró, Phys. Rev. B **61**, 9752 (2000).
- ¹⁷ Y. Gallais, A. Sacuto, T. P. Devereaux, and D. Colson, Phys. Rev. B **71**, 012506 (2005).
- ¹⁸ S. Sakai, S. Blanc, M. Civelli, Y. Gallais, M. Cazayous, M.-A. Méasson, J. S. Wen, Z. J. Xu, G. D. Gu, G. Sangiovanni, Y. Motome, K. Held, A. Sacuto, A. Georges, and M. Imada, Phys. Rev. Lett. **111**, 107001 (2013).
- ¹⁹ Zhihao Geng and Shiping Feng, Phys. Lett. A **375**, 214 (2010).
- ²⁰ B. Muschler, W. Prestel, E. Schachinger, J. P. Carbotte, R. Hackl, Shimpei Ono, Yoichi Ando, J. Phys.: Condens. Matter **22**, 375702 (2010).
- ²¹ A. V. Chubukov, T. P. Devereaux, and M. V. Klein, Phys. Rev. B **73**, 094512 (2006).
- ²² D. Manske, C. T. Rieck, R. Das Sharma, A. Bock, and D. Fay, Phys. Rev. B **56**, R2940(R) (1997).
- ²³ D. Branch and J. P. Carbotte, Phys. Rev. B **52**, 603 (1995).
- ²⁴ T. P. Devereaux, D. Einzel, B. Stadlober, R. Hackl, D. H. Leach, and J. J. Neumeier, Phys. Rev. Lett. **72**, 396 (1994).
- ²⁵ Shiping Feng, Phys. Rev. B **68**, 184501 (2003); Shiping Feng, Tianxing Ma, and Huaiming Guo, Physica C **436**, 14 (2006).
- ²⁶ Shiping Feng, Huaisong Zhao, and Zheyu Huang, Phys. Rev. B. **85**, 054509 (2012).
- ²⁷ See, e.g., the review, Shiping Feng, Yu Lan, Huaisong Zhao, Lülin Kuang, Ling Qin, and Xixiao Ma, Int. J. Mod. Phys. B **29**, 1530009 (2015).
- ²⁸ Nan Lin, Emanuel Gull, and Andrew J. Millis, Phys. Rev. Lett. **109**, 106401 (2012).
- ²⁹ Dominic Bergeron, Vasyl Hankevych, Bumsoo Kyung, and A.-M. S. Tremblay, Phys. Rev. B **84**, 085128 (2011).
- ³⁰ P. W. Anderson, Science **235**, 1196 (1987).
- ³¹ See, e.g., the review, Philip Phillips, Rev. Mod. Phys. **82**, 1719 (2010).
- ³² See, e.g., the review, P. A. Lee, N. Nagaosa, and X.-G. Wen, Rev. Mod. Phys. **78**, 17 (2006).
- ³³ Shiping Feng, J. B. Wu, Z. B. Su, and L. Yu, Phys. Rev. B **47**, 15192 (1993).
- ³⁴ L. Zhang, J. K. Jain, and V. J. Emery, Phys. Rev. B **47**, 3368 (1993).
- ³⁵ See, e.g., the review, L. Yu, in *Recent Progress in Many-Body Theories*, edited by T. L. Ainsworth, C. E. Campbell, B. E. Clements, and E. Krotscheck (Plenum, New York, 1992), Vol. **3**, p. 157.
- ³⁶ P. W. Anderson, Science **288**, 480 (2000).
- ³⁷ Shiping Feng, Jihong Qin, and Tianxing Ma, J. Phys.: Condens. Matter **16**, 343 (2004); Shiping Feng, Z.B. Su, and L. Yu, Phys. Rev. B **49**, 2368 (1994).
- ³⁸ Shiping Feng, Lülin Kuang, and Huaisong Zhao, Physica C **517**, 5 (2015).
- ³⁹ See, e.g., the review, Riccardo Comin, Andrea Damascelli, Annu. Rev. Condens. Matter Phys. **7**, 369 (2016).
- ⁴⁰ R. Comin, A. Frano, M. M. Yee, Y. Yoshida, H. Eisaki, E. Schierle, E. Weschke, R. Sutarto, F. He, A. Soumyanarayanan, Yang He, M. Le Tacon, I. S. Elfimov, Jennifer E. Hoffman, G. A. Sawatzky, B. Keimer, and A. Damascelli, Science **343**, 390 (2014).
- ⁴¹ R. Comin, R. Sutarto, F. He, E. H. da Silva Neto, L. Chauviere, A. Fraño, R. Liang, W. N. Hardy, D. A. Bonn, Y. Yoshida, H. Eisaki, A. J. Achkar, D. G. Hawthorn, B. Keimer, G. A. Sawatzky, and A. Damascelli, Nat. Mater. **14**, 796 (2015).
- ⁴² G. Campi, A. Bianconi, N. Poccia, G. Bianconi, L. Barba, G. Arrighetti, D. Innocenti, J. Karpinski, N. D. Zhigadlo, S. M. Kazakov, M. Burghammer, M. v. Zimmermann, M. Sprung, and A. Ricci, Nature **525**, 359 (2015)
- ⁴³ N. Harrison and S. E. Sebastian, New J. Phys. **16**, 063025 (2014).
- ⁴⁴ W. A. Atkinson, A. P. Kampf, and S. Bulut, New J. Phys. **17**, 013025 (2015).
- ⁴⁵ Shiping Feng, Deheng Gao, and Huaisong Zhao, Phil. Mag. **96**, 1245 (2016); Huaisong Zhao, Deheng Gao, and Shiping Feng, Physica C **534**, 1 (2017).
- ⁴⁶ Itzik Kapon, David S. Ellis, Gil Drachuck, Galina Bazalitski, Eugen Weschke, Enrico Schierle, Jörg Stempffer, Christof Niedermayer, and Amit Keren, arXiv:1612.06864.